Upconversion Luminescence Resonance Energy Transfer (LRET)-Based Biosensor for Rapid and Ultrasensitive Detection of Avian Influenza Virus H7 Subtype

ARTICLE *in* SMALL · JUNE 2014

Impact Factor: 8.37 · DOI: 10.1002/smll.201303766

5 AUTHORS, INCLUDING:

W.W. Ye
The Hong Kong Polytechnic University
21 PUBLICATIONS **212** CITATIONS
SEE PROFILE

Mingkiu Tsang
The Hong Kong Polytechnic University
15 PUBLICATIONS **271** CITATIONS
SEE PROFILE

mo Yang
University of Shanghai for Science and Tec…
166 PUBLICATIONS **1,586** CITATIONS
SEE PROFILE

small
NANO MICRO

Biosensors

Upconversion Luminescence Resonance Energy Transfer (LRET)-Based Biosensor for Rapid and Ultrasensitive Detection of Avian Influenza Virus H7 Subtype

Wei Wei Ye, Ming-Kiu Tsang, Xuan Liu, Mo Yang, and Jianhua Hao**

***A**vian influenza viruses (AIV) with good adaptation and various mutations have threatened both human and animals' health. The H7 subtypes have the potential to cause pandemic threats to human health due to the highly pathogenic characteristics. Therefore, it is quite urgent to develop a novel biosensor for rapid and sensitive detection of H7 subtypes. In this work, a biosensor based on luminescence resonance energy transfer (LRET) from $BaGdF_5$:Yb/Er upconversion nanoparticles (UCNPs) to gold nanoparticles (AuNPs) has been developed for rapid and sensitive H7 subtypes detection. The amino modified capture oligonucleotide probes are covalently linked to poly(ethylenimine) (PEI) modified $BaGdF_5$:Yb/Er UCNPs. The thiol modified oligonucleotides with H7 hemagglutinin gene sequence are conjugated to surfaces of AuNPs. The hybridization process between complementary strands of H7 Hemagglutinin gene and its probe brings the energy donor and acceptor into close proximity, leading to the quenching of fluorescence of UCNPs. A linear response is obtained ranging from 10 pM to 10 nM and the limit of detection (LOD) is around 7 pM with detection time around 2 hours. This biosensor is expected to be a valuable diagnostic tool for rapid and sensitive detection of AIV.*

1. Introduction

Avian influenza viruses (AIV) have become an increased threat for both humans and animals. AIV consist of two viral surface glycoproteins, hemagglutinin (HA) and neuraminidase (NA), forming multiple distinct virus subtypes of 16 HA and 9 NA subtypes.[1,2] Among them, influenza A H7 subtypes are characterized as highly pathogenic avian influenza and have the capacity to cause pandemic threats to human health.[3] For example, the influenza A virus subtype H7N9 emerged in south eastern China in March 2013 and the reported number of human infections was more than 130.[4] The infected people presented with rapidly progressing lower respiratory tract infections.[5] H7 is the major antigen of the H7N9 AIV, and plays an important role in mediating viral replication cycle, receptor binding and membrane fusion.[6] The early and rapid detection of H7 subtypes is of great importance for preventing infection in poultry and reducing the risk of a potential pandemic in human.

The conventional method for AIV detection and subtype identification is based on virus isolation, which is sensitive but suffers from time-consuming and labor-intensive procedures.[7] Enzyme-linked immunosorbent assay (ELISA) is a rapid method, but has relatively low sensitivities.[8] Target

W. W. Ye,[+] Prof. M. Yang
Interdisciplinary Division of Biomedical Engineering
the Hong Kong Polytechnic University
Hung Hom, Kowloon, Hong Kong, P. R. China
E-mail: Mo.Yang@polyu.edu.hk
M.-K. Tsang,[+] Prof. J. H. Hao
Department of Applied Physics
the Hong Kong Polytechnic University
Hung Hom, Kowloon, Hong Kong, P. R. China
E-mail: jh.hao@polyu.edu.hk
X. Liu
Institute of Textiles & Clothing
the Hong Kong Polytechnic University
Hung Hom, Kowloon, Hong Kong, P. R. China
[+]These authors contributed equally to this work

DOI: 10.1002/smll.201303766

amplification methods such as reverse transcription-PCR (RT-PCR) has been widely implemented for AIV detection, but the need for expensive equipments, trained personals, relatively long testing time and susceptible to contamination during amplification process limits their application for on-site detection.[9,10] Therefore, developments of biosensors with high sensitivity are needed to enable rapid detection of AIV with high sensitivity in a cost-effective way. Recently, various biosensors have been developed for direct detection of AIV genes including silicon nanowire based field-effect transistor,[11] gold nanoparticle based genomic microarray assay,[12] impedimetric sensor,[13] and magnetic electrochemical array.[14] These biosensors are based on hybridizaiton between target viral nucleic acid and capture oligonucleotide probe immobilized on biosensor substrates in the absence of target amplification, which can provide rapid response and ultra-sensitivity for AIV detection.

Förster resonance energy transfer (FRET), a direct and sensitive technology, has been widely used for bioassay, biosensing, bioimaging, and photodynamic therapy.[15–17] The FRET biosensor generally consists of an acceptor fluorophore and a donor fluorophore and can be classified into intermolecular and intramolecular types.[18,19] Traditional fluorophore includes FAM, Texas red, Cy5 which are limited by high cost and photobleaching. Therefore, they are not suitable for developing reliable and low cost biosensor. It is known that lanthanide-based upconversion nanoparticles (UCNPs) can convert low-energy near-infrared (NIR) photons into visible emission by sequentially absorbing multiple photons and energy transfer which is named as luminescence resonance energy transfer (LRET).[20] Additionally, UCNPs have attracted great interest owing to their merits, such as photostability, low toxicity, and biocompatibility.[21–24] Among different upconversion hosts, fluorides are promising host materials because they possess low phonon energy and therefore fluoride-based UCNPs have been reported extensively, such as $BaYF_5$, $NaYF_4$, KYF_4 and $NaLuF_4$.[25–28] Recently, UCNPs based LRET biosensors have demonstrated promising applications in detecting biomolecules, such as glutathione, DNA and avidin.[29–31] A time-resolved LRET biosensor based on amine-functionalized lanthanide-doped $NaYF_4$ UCNPs has been developed for the detection of avidin.[32] This biosensor achieved a detection limit of about 5 nM and eliminated the interference of short-lived background fluorescence time-resolved detection. Also, the $NaYF_4$ UCNPs are prepared by facile hydrothermal synthesis. As a result, this biosensor features advantages, such as low cost, simple and fast readout. However, the detection limit needs to be improved to meet ultrasensitive detection of biomolecules applications. Very recently, $BaGdF_5$ UCNPs have demonstrated promising remarkable multi-modal bioimaging.[33] However, there is limited report about $BaGdF_5$ UCNPs-based LRET biosensors.

Gold nanoparticles (AuNPs) possess quantization effects due to the confinement of electron movement, which leads to discrete electron transition energy levels. Therefore, surface plasmon resonance (SPR) phenomena are observed for AuNPs.[34] SPR is the result of collective resonant oscillation of free electrons on AuNPs surface excited by the incoming photons. Owing to the strong surface plasma absorption in the NIR-to-IR region, AuNPs are good acceptors in a LRET system. Moreover, AuNPs have larger absorption surface area and longer working distance compared with classical dye quenchers, which hence improves the quenching efficiency.[35]

In this work, a $BaGdF_5$:Yb/Er UCNPs-based LRET biosensor has been developed for influenza A H7 subtype detection, with $BaGdF_5$:Yb/Er UCNPs and AuNPs as energy donor-acceptor pairs. Capture oligonucleotide probe was designed based on sequence specific for hemaglutinin (HA) genes of H7 virus subtypes and conjugated to poly(ethylenimine) (PEI) modified UCNPs. AuNPs were then conjugated with H7 hemaglutinin gene oligonucleotides. The LRET process was initiated by the hybridization between complimentary oligonucleotide pairs. Due to the NIR absorption characteristic of $BaGdF_5$:Yb/Er UCNPS, the upconversion emission was quenched by AuNPs, which could be used to quantify H7 oligonucleotide target. In combination of high fluorescence emission capability of UCNPs and the high quenching efficiency of AuNPs, a low limit of detection of 7 pM with detection time around 2 hours was achieved for H7 target oligonucleotides. As a result, this LRET biosensor has the potential to be used for ultrasensitive detection of avian influenza viruses in clinical diagnostics.

2. Results and Discussion

2.1. Design of LRET Sensor for H7 Hemagglutinin Gene Detection

The principle of H7 hemagglutinin gene detection by upconversion $BaGdF_5$:Yb/Er UCNPs and AuNPs based LRET biosensor is shown in **Figure 1**. AuNPs and UCNPs acted as the acceptor and donor of LRET pair, respectively. PEI modified UCNPs were conjugated with amine modified oligonucleotide probe while AuNPs were conjugated with target oligonucleotides (H7 hemagglutinin gene segment). Oligonucleotide hybridization between complimentary pairs brought UCNPs and AuNPs into close proximity. Under 980 nm laser excitation, the upconversion emission of UCNPs was absorbed by AuNPs. By measuring the photoluminescence intensity change of the solution, the H7 hemagglutinin gene can be detected.

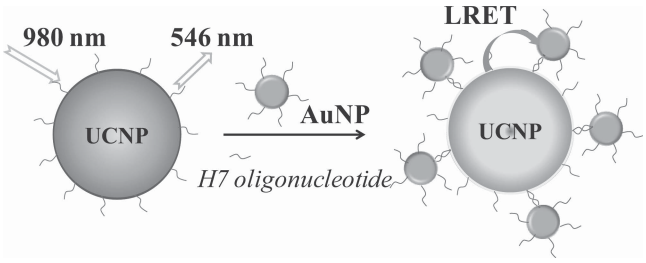

Figure 1. Schematic diagram of H7 hemagglutinin gene detection by LRET biosensor based on energy transfer from $BaGdF_5$:Yb/Er UCNPs to AuNPs.

small 2014,
DOI: 10.1002/smll.201303766

NANO MICRO small

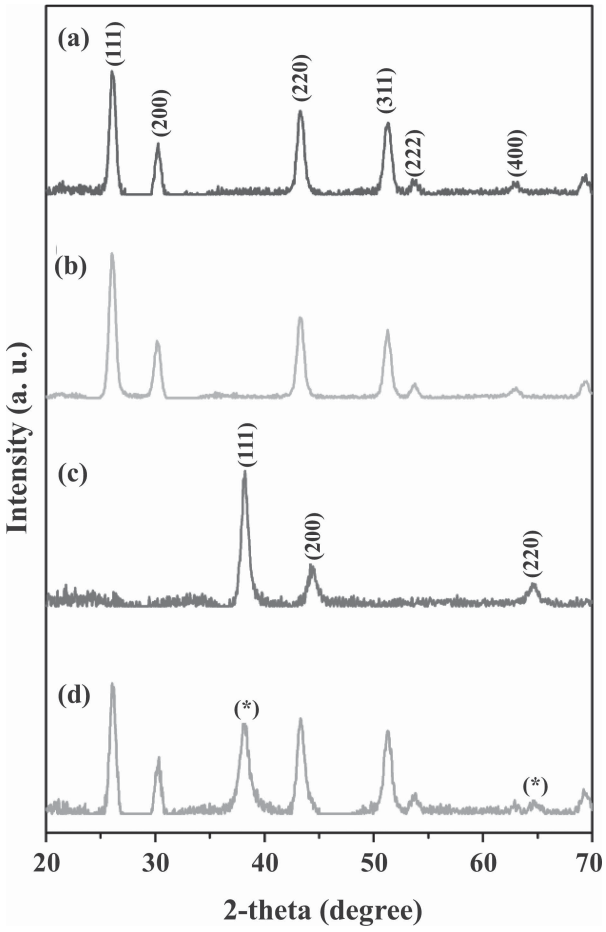

Figure 2. XRD pattern of the (a) $BaGdF_5$:Yb/Er UCNPs, (b) $BaGdF_5$:Yb/Er UCNPs-oligo, (c) AuNPs, and (d) $BaGdF_5$:Yb/Er UCNPs-oligo-AuNPs.

2.2. Structural and Phase Characterizations of $BaGdF_5$:Yb/Er UCNPs and AuNPs

The PEI-modified $BaGdF_5$:Yb/Er UCNPs were synthesized by one-pot hydrothermal method with PEI as capping ligand. X-ray diffraction (XRD) is used to characterize the phase composition of as-synthesized $BaGdF_5$ UCNPs (**Figure 2**). The XRD pattern of PEI-modified $BaGdF_5$:Yb/Er UCNPs is shown in Figure 2a. The pattern is well matched with the standard pattern of cubic phase $BaGdF_5$ (JCPDS 24-0098) and therefore the as-synthesized $BaGdF_5$ UCNPs possess pure cubic phase structure. As shown in Figure 2b, the XRD pattern of the $BaGdF_5$ UCNPs does not change after conjugating with oligonucleotide and hence the conjugation does not change the phase structure of UCNPs. Moreover, the structure of citrate-stabilized AuNPs is also characterized by XRD in Figure 2c. The diffracted peaks indexed with the standard pattern of gold (JCPDS 04-0784) confirm the cubic phase structure of AuNPs.[36] After oligonucleotide hybridization, AuNPs are linked to $BaGdF_5$ UCNPs, Figure 2d depicts the XRD pattern of the as-conjugated sample. The diffraction peaks of $BaGdF_5$ and AuNPs are observed (AuNPs XRD peaks are denoted by asterisks), which indicate the successful conjugation of AuNPs on $BaGdF_5$ UCNPs. Owing to the close diffraction angles of (200) $BaGdF_5$ and (220) Au, the two peaks at about 43° to 44° overlapped as one peak.

TEM was performed to investigate the size and morphology of the as-prepared $BaGdF_5$:Yb/Er UCNPs, $BaGdF_5$:Yb/Er UCNPs-oligo conjugation, and $BaGdF_5$:Yb/Er UCNPs-oligo conjugation with AuNPs by complimentary oligonucleotide probe (**Figure 3**). The $BaGdF_5$:Yb/Er UCNPs were synthesized by a one-step hydrothermal synthesis with PEI as surfactant to enhance monodispersity in water. Figure 3a indicates the PEI modified BaGdF5 UCNPs have good monodispersity in water . The monodispersity could be improved by performing ligand exchange of the UCNPs obtained in thermal decomposition.[37,38] However, thermal decomposition requires high reaction temperature and yields hydrophobic UCNPs. Therefore, the preparation of UCNPs will be costly and laborious. Currently, the water dispersity may be improved by synthesizing core-shell structure with SiO_2 and $BaGdF_5$:Yb/Er UCNPs as shell and core respectively because SiO_2 shell based core-shell UCNPs are well-known to possess promising hydrophilic property.[39] The selected area electron diffraction (SAED) pattern in Figure 3b indicates the cubic structure of $BaGdF_5$. This observation is consistent with the aforementioned XRD analysis (Figure 2a). Moreover, the average size of the $BaGdF_5$ UCNPs is about 14 nm (Figure 3c). From the high resolution TEM (HRTEM) image (Figure 3e), the d-spacing of a single $BaGdF_5$ UCNPs was measured to be about 2.16 Å and this value is close to the d-spacing of (220) plane of cubic $BaGdF_5$, which confirms good crystallinity of $BaGdF_5$:Yb/Er UCNPs. In addition, the chemical composition of oligonucleotide capped $BaGdF_5$ UCNPs was verified by energy dispersive X-ray (EDX), the EDX spectrum (Figure 3d) indicates the presence of Ba, Gd, F, O and P. The first three elements are due to presence of $BaGdF_5$:Yb/Er UCNPs while Yb and Er are not detected because of low doping concentration. Importantly, the existence of O and P is evident for the coating of oligonucleotide on the surface of $BaGdF_5$:Yb/Er UCNPs. However, it should be noted that the Cu peaks in the spectrum are due to the copper grid for TEM sample. The HRTEM in Figure 3f shows a single oligonucleotide conjugated $BaGdF_5$:Yb/Er UCNP and an about 2 nm thick layer of oligonucleotide around UCNPs is observed. Therefore, this observation supports the EDX result. In Figure 3g and h, the $BaGdF_5$:Yb/Er UCNPs are surrounded by numerous AuNPs to form a satellite structure, which demonstrates the assembly between UCNPs and AuNPs through oligonucleotide hybridization.

2.3. UC Spectra of UCNPs-oligo and Absorption Spectra of AuNPs-Oligo

The PEI-modified $BaGdF_5$:Yb/Er UCNPs are readily dispersed in water to form a colloidal solution. Under 980 nm laser illumination, the $BaGdF_5$:Yb/Er UCNPs emits intense green upconversion emission (inset of **Figure 4**) and the green emission is attributed to the existence of the emission bands centered at 520, 540 and 654 nm (Figure 4). After

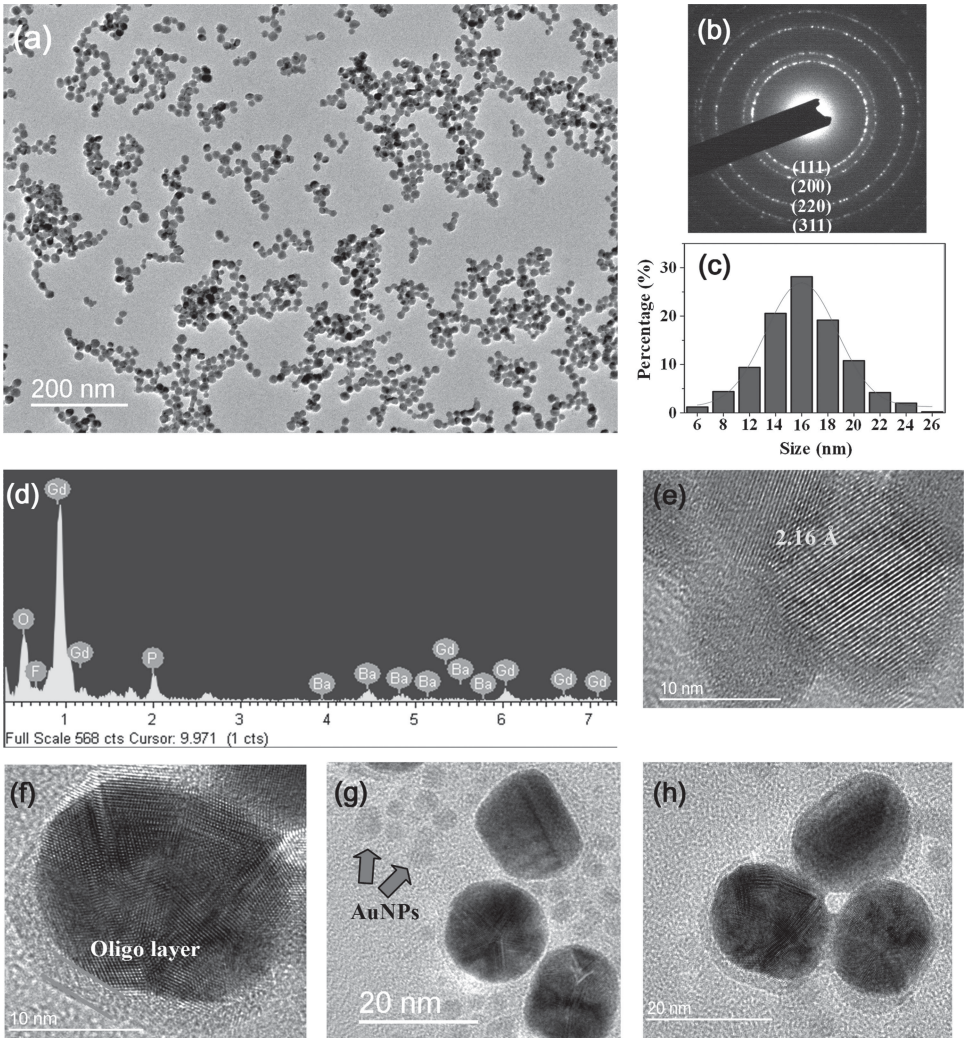

Figure 3. (a) TEM image (b) SAED pattern (c) Size distribution of as-prepared PEI-modified $BaGdF_5$:Yb/Er UCNPs; (d) EDX of oligonucleotide conjugated $BaGdF_5$:Yb/Er UCNPs; HRTEM of (e) PEI-modified $BaGdF_5$:Yb/Er UCNPs (f) oligonucleotide conjugated $BaGdF_5$:Yb/Er UCNPs; (g) and (h) oligonucleotide conjugated $BaGdF_5$:Yb/Er UCNPs assembled with AuNPs.

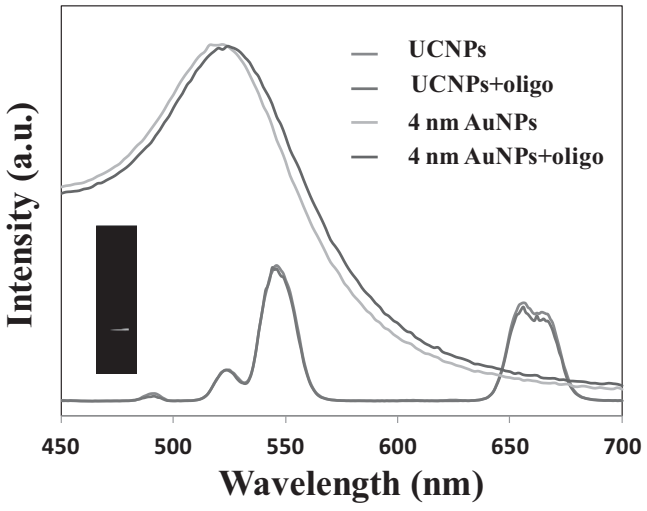

Figure 4. UC emission spectra of $BaGdF_5$:Yb/Er UCNPs and oligonucleotide coated $BaGdF_5$:Yb/Er UCNPs in water under 980 nm laser excitation, and UV-Vis absorption spectra of AuNPs and AuNPs-oligo (Inset: green UC emission of $BaGdF_5$:Yb/Er UCNPs).

conjugation of $BaGdF_5$:Yb/Er UCNPs with oligonucleotide, the upconversion emission does not change due to coating while the emission intensity shows slight drop due to the oligonucleotide coating. In the absorption spectra of AuNPs with average diameter of 4 nm, the main absorption peaks are mainly in the range of 520–550 nm. When AuNPs were conjugated with H7 target oligonucleotides, the absorption peak shifted slightly towards right. Herein, the spectral overlapping between UC emission of $BaGdF_5$:Yb/Er UCNPs and absorption characteristic of AuNPs manifests the LRET efficiency of this sensor.

Conjugation of oligonucleotide onto $BaGdF_5$:Yb/Er UCNPs was further confirmed by the appearance of the characteristic vibration bands of guanine base (1688 cm^{-1}), cytosine base (1530 cm^{-1}), thymine base (1280 cm^{-1}) and sugar phosphate (1250-850 cm^{-1}) in the FTIR spectrum (Figure S3).[40] Zeta potential measurements showed that BaGdF5:Yb/Er UCNPs were highly negatively charged after oligonucleotide conjugation with average potential –24.2 mV which was due to the negative charges carried by conjugated oligonucleotides (Figure S4).

small 2014,
DOI: 10.1002/smll.201303766

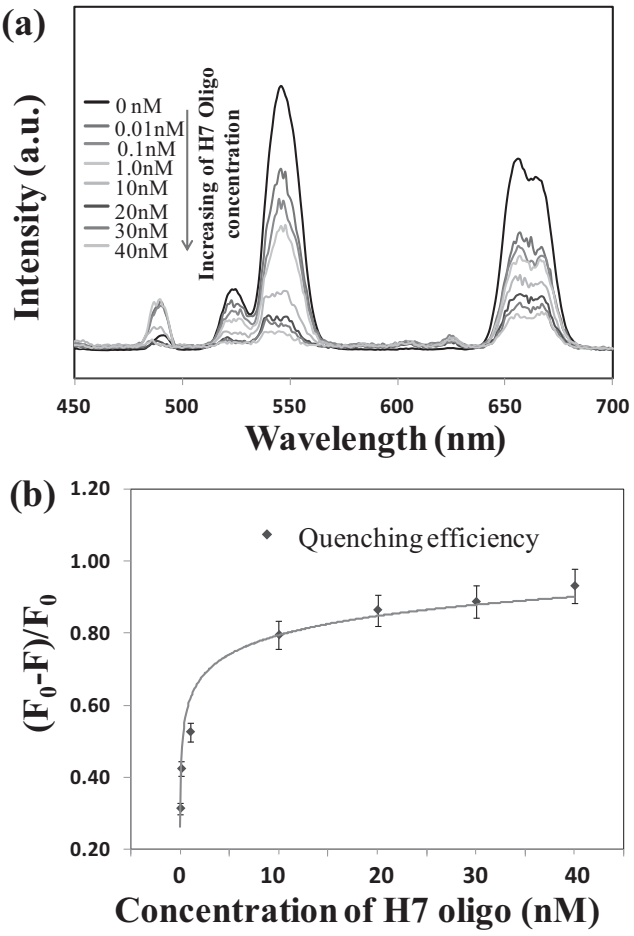

Figure 5. (a) Luminescence spectra of UCNPs-oligo with various concentrations of H7 target oligonucleotides conjugated with AuNPs; (b) quenching efficiency change with concentrations of H7 target oligonucleotides.

2.4. Construction of UCNPs-Oligo-AuNPs LRET System

Figure 5 shows the luminescence spectra of PEI-modified $BaGdF_5$:Yb/Er UCNPs with addition of various concentrations of AuNPs with complimentary H7 oligonucleotides. Herein, a fixed amount of $BaGdF_5$:Yb/Er UCNPs with concentration of 0.2 mg/mL was used. By using fluorescently labeling method or UV-Vis spectroscopy characterization, the surface density of oligonucleotides was estimated to be 10 oligonucleotides per AuNP. Therefore, H7 oligonucleotide concentration could be calculated based on this ratio. After 2 hours incubation for hybridization, upconversion spectra were measured. As shown in Figure 5a, the fluorescence signals decreased gradually with increasing concentrations of H7 oligonucleotides. As a result of hybridization between H7 oligonucleotide targets on AuNPs and the complimentary oligonucleotide probes on UCNPs, luminescence quenching was realized. It was observed that both peak values at 540 nm and 654 nm decreased with increasing concentrations of H7 oligonucleotides due to the strong quenching capability of AuNPs. Therefore, ratiometric luminescence method is not suitable for this LRET system which needs an emission peak without obvious change as an internal standard.[41,42] As shown in Figure 5b, the quenching efficiency reached a maximum of 88% with 20 nM H7 oligonucleotides. The quenching efficiency almost unchanged when H7 oligonucleotide concentration further increased. The quenching efficiency of 88% was quite high due to the strong quenching capability of AuNPs. It was also observed that the linear response range was under 10 nM in Figure 5b. The decay profiles of UCNPs-oligo emission at 540 nm before and after AuNPs-oligo conjugation were measured using 980-nm laser pulses (Figure S5). The luminescence life time was observed to be shortened by conjugation with AuNPs which demonstrated this process was mainly due to the non-radiative LRET effect.[39,43]

To investigate the limit of detection (LOD) of this LRET sensor, further experiments were performed with low concentrations of H7 oligonucleotides from 1 pM to 10 nM. **Figure 6**a shows the fluorescence signal quenching (F_0-F) due to LRET quenching versus H7 oligonucleotide concentrations. The quenching effect was decreased with the decreasing of H7 oligonucleotide concentrations. The limit of detection (LOD) was determined by the control signal plus three times of noise signal (standard derivation) which was

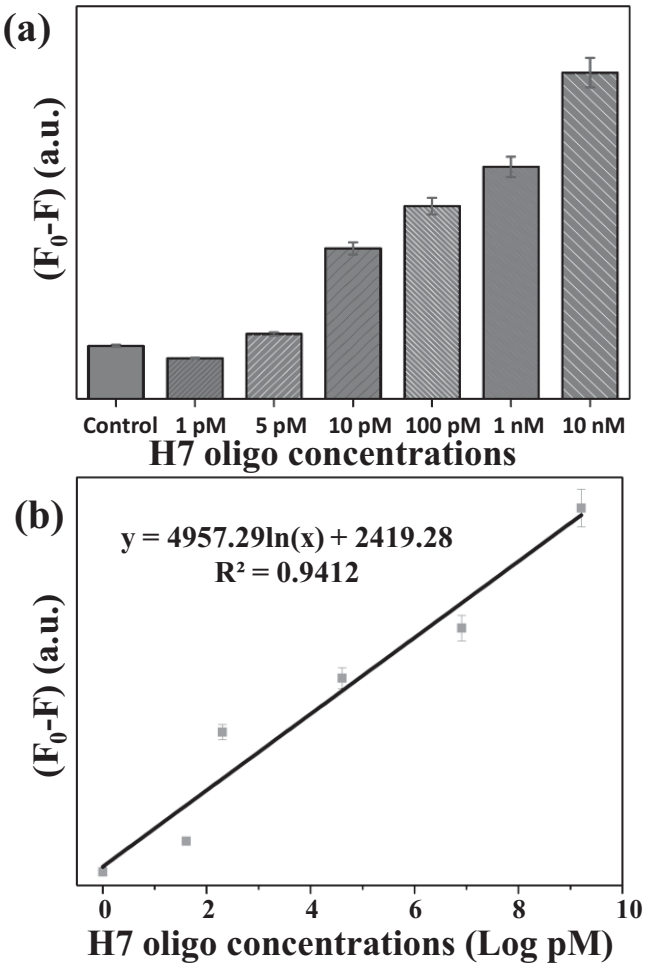

Figure 6. (a) Luminescence signal quenching (F_0-F) versus H7 gene oligonucleotide concentrations from 1 pM to 10 nM. (b) Linear relationship between luminescence signal quenching and concentrations of H7 oligonucleotides in the range between 1 pM to 10 nM as y = 4957.29 ln(x) + 2419.28, with R^2 = 0.9412.

DOI: 10.1002/smll.201303766

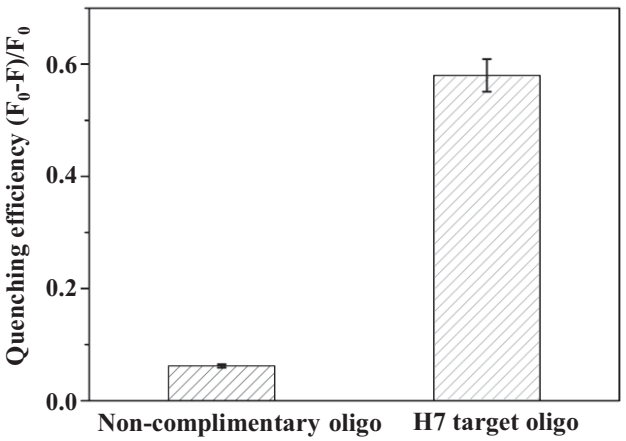

Figure 7. Comparison of quenching efficiency between noncomplementary oligonucleotides and complementary H7 target oligonucleotides.

calculated to be 7 pM. Figure 6b shows a linear relationship between luminescence signal quenching degree and concentrations of H7 oligonucleotides in the range between 1 pM to 10 nM as $y = 4957.29 \ln(x) + 2419.28$, with $R^2 = 0.9412$.

To investigate the specificity of this LRET system, 6 nM noncomplementary oligonucleotides and 6 nM H7 oligonucleotides were tested with the same procedures as the above experiments. As shown in in **Figure 7**, the quenching efficiency of AuNPs conjugated with noncomplementary oligonucleotides was much lower than that of AuNPs conjugated with the complementary H7 target oligonucleotides, which demonstrated the specificity of this LRET biosensor.

3. Conclusion

In summary, an upconversion luminescence resonance energy transfer (LRET) biosensor based on $BaGdF_5$:Yb/Er UCNPs and AuNPs has been successfully developed for rapid detection of H7 hemagglutinin genes of avian influenza viruses. PEI-modified $BaGdF_5$:Yb/Er UCNPs were synthesized by one-step hydrothermal synthesis and conjugated with amino modified capture oligonucleotides. Once UCNPs-oligo captured AuNPs conjugated with H7 target oligonucleotides, the green UC emission of UCNPs is quenched due to the absorption characteristics of AuNPs at 540 nm. By quantifying the quenching effieficency, both the identity and quantity of H7 hemagglutinin genes can be determined. This system has a remarkably low limit of detection of 7 pM with the detection time around 2 hours, and a linear working range from 10 pM to 10 nM. This LRET sensor features simplicity, fast readout and low cost. Therefore, this UCNPs and AuNPs based LRET system could be extended to other biomolecule detection with high sensitivity and selectivity.

4. Experimental Section

Materials: $Ln(NO_3)_3 \cdot 6H_2O$ (Ln = Gd, Yb, Er) were purchased from Sigma Aldrich and dissolved in de-ionized water (DI-water) to form solution with concentrations of 0.5 M $Gd(NO_3)_3$, $Yb(NO_3)_3$ and 0.1 M $Er(NO_3)_3$. Ethylene glycol (EG, 99%) and branched polyethylenimine (PEI, 25 kDa) were purchased from Sigma-Aldrich. NH_4F (99.99%) and $BaCl_2$ (99.99%) were obtained from Sinopharm Chemical Reagent Co., China. Gold (III) chloride trihydrate ($HAuCl_4 \cdot 3H_2O$ and sodium citrate solution were purchased from Sigma Aldrich. All of these chemicals were used as received without further purification.

One-pot Hydrothermal Synthesis of PEI-modified $BaGdF_5$:Yb/Er UCNPs: Hydrophilic PEI-modified $BaGdF_5$:Yb/Er UCNPs with high monodispersity were synthesized using the hydrothermal synthesis method.[33] Typically, 1.0 g of PEI was added to 20 ml of EG with 1 mmol of lanthanide dopants, 0.5 M $Gd(NO_3)_3$, $Yb(NO_3)_3$ and 0.1 M $Er(NO_3)_3$ with a molar ratio of 78:20:2 under vigorous mixing. After that, 1 mmol of $BaCl_2$ was added to the above solution. The mixture was stirred for 30 minutes to form a transparent homogenous solution. Then, 5.5 mmol of NH_4F in 10 ml of EG was added to the above mixture. The mixture was agitated for another 1 h and transferred to a 50 ml stainless steel Telfon-lined autoclave and kept at 190 °C for 24 h. After reaction, the as-synthesized UCNPs were separated from the reaction mixture by centrifugation, washed several times by ethanol and DI-water. Finally, the UCNPs were dried in vacuum at 60°C for 24 h.

Preparation of Gold Nanoparticles (AuNPs): The procedures described by Grabar et al. was followed for the preparation of gold nanoparticles.[44] Briefly, a mixture of $HAuCl_4$ (3 μL, 14.3 wt %) and DI water (10 ml) were transferred to a clean beaker, which was thoroughly washed in aqua regia (mixture of HCl and HNO_3 with the ratio of 3:1) and rinsed in DI water. With vigorous stirring, sodium citrate solution (1 ml, 1 wt %) was added to the boiling solution within one second. The solution color changed from pale yellow to wine red in a few minutes and continued to boil for 15 minutes. It was left to cool down to room temperature by stirring.

Characterizations: Powder X-ray diffraction (XRD) patterns of the as-prepared UCNPs were recorded using a Rigaku smart lab 9 kW (Rigaku, Japan) with Cu Kα radiation (λ = 1.5406 Å). The shape, size and structure of the as-prepared $BaGdF_5$:Yb/Er UCNPs and AuNPs were characterized using a JEOL-2100F transmission electron microscopy (TEM) equipped with an Oxford Instrument EDS system, operating at 200 kV. Samples for TEM were prepared on holey carbon coated 400 mesh copper grids. Fourier transform infrared spectrum (FTIR) was recorded by a PerkinElmer Spectrum 100 FT-IR spectrometer (PerkinElmer Inc., USA). Zeta potential measurements were performed on a ZetaPlus Zeta Potential Analyzer (Brookhaven Instruments Corp., USA). Upconversion spectra were recorded using FLS920P Edinburgh analytical instrument apparatus equipped with a CW 980 nm diode laser as an excitation source.

AuNPs-oligo Conjugation: Thiol modified H7 hemagglutinin oligonucleotide (H7: 5′-thiol-AGATAATGCTGCATTCCCGCAGATG-3′, a 25-base fragment of influenza virus H7 gene sequence from an AIV isolate A/Hangzhou/1/2013 strain, genbank accession no. KC853766) and another non-target oligonucleotide (S1: 5′-thiol-ACATCATAGCAGGCTAGGTTGGTCG-3′) were synthesized by Integrated DNA Technologies (IDT) Inc. (Coralville, IA). Thiol modified oligonucleotide was treated with DTT (0.1 M, pH 8.2) for 30 minutes to cleave disulfur linkage. The activated H7 oligonucleotides were purified by gel columns (illustra MicroSpin G-25 Columns, GE Healthcare, UK) based on the manufacturer's instructions

small 2014,
DOI: 10.1002/smll.201303766

NANO MICRO small

and characterized by UV-visible spectrophotometer (Ultrospec 2100 pro). After mixing of purified H7 oligonucleotides with AuNPs (600 µl) and incubation for 24 h at room temperature, sodium solution (0.1 M NaCl, 5 mM NaH_2PO_4) was added to age for 16 hours. It was centrifuged for 30 minutes at a high speed 13,200 rpm. The remaining red oily precipitate at the bottom was collected and washed by PBS three times (3 × 600 µl) to remove excess thiol modified H7 oligonucleotides. Finally, It was suspended in PBS (600 µl) and characterized by the UV-Vis absorption spectra.

Conjugation of the Probe Oligo to $BaGdF_5$:Yb/Er UCNPs: Amino modified oligonucleotide probe (5′-amino-CATCTGCGGGAATGCAGCATTATCT-3′) was covalently conjugated with $BaGdF_5$:Yb/Er UCNPs using glutaraldehyde as the cross-linking agent. 2 mg of PEI modified UCNPs was dissolved in 200 µl of PBS (pH 7.4, 10 mM), followed by adding 2 µl of glutaraldehyde (Grade II, 25% in H_2O, Sigma Aldrich) to the mixture. After shaking for reaction with 1 hour at room temperature, it was centrifuged and washed by PBS 3 times to remove excess glutaraldehyde and resuspended in 200 µl PBS solution. The glutaraldehyde-activated UCNPs were incubated with amino modified oligonucleotide (100 µM) with gentle shaking overnight at room temperature. The mixture was centrifuged and the content of UCNPs-oligo was collected from the bottom. After filtering to remove excess oligonucleotide, the UCNPs-oligo conjugation was diluted in 400 µl PBS and stored at 4 °C for further use.

Upconversion Quenching: To investigate the luminescence quenching efficiency, a fixed amount of $BaGdF_5$:Yb/Er UCNPs-oligo (0.2 mg/mL) was incubated with various concentrations of AuNPs conjugated with H7 oligos for 2 h at room temperature to ensure complete hybridization. After adjusting the total volume of solution to 1 mL with DI water, the mixtures were used for LRET measurement. The upconversion LRET spectra were obtained using FLS920P Edinburgh analytical instrument apparatus equipped with a CW 980 nm diode laser as an excitation source. All upconversion luminescence spectra were recorded under the same condition.

Supporting Information

Supporting Information is available from the Wiley Online Library or from the author.

Acknowledgements

This work was supported by the Hong Kong Ph. D Fellowship Scheme Fund (HKPF10-13386/ PolyU RUY5).

[1] J. J. Skehel, D. C. Wiley, *Annu. Rev. Biochem.* **2000**, *69*, 531.
[2] M. N. Matrosovich, T. Y. Matrosovich, T. Gray, N. A. Roberts, H. Klenk, *J. Virol.* **2004**, *78*, 12665.
[3] J. A. Belser, C. B. Bridges, J. M. Katz, T. M. Tumpey, *Emerging Infectious Diseases* **2009**, *15*, 859.
[4] M. Hvistendahl, D. Normile, J. Cohen, *Science* **2013**, *340*, 414.
[5] R. Gao, B. Cao, Y. Hu, Z. Feng, D. Wang, W. Hu, J. Chen, Z. Jie, H. Qiu, K. Xu, *N. Engl. J. Med.* **2013**, *368*, 1888.
[6] R. Wagner, A. Herwig, N. Azzouz, H. D. Klenk, *J. Virol.* **2005**, *79*, 6449.
[7] Y. Amano, Q. Cheng, *Anal. Bioanal. Chem.* **2005**, *381*, 156.
[8] S. Grund, S. Pietzonka, S. Michel, O. Adams, *J. Virol. Methods* **2013**, *193*, 558.
[9] B. Hoffmann, T. Harder, E. Starick, K. Depner, O. Werner, M. Beer, *J. Clin. Microbiol.* **2007**, *45*, 600.
[10] I. Monne, S. Ormelli, A. Salviato, C. De Battisti, F. Bettini, A. Salomoni, A. Drago, B. Zecchin, I. Capua, G. Cattoli, *J. Clin. Microbiol.* **2008**, *46*, 1769.
[11] C. H. Lin, C. H. Hung, C. Y. Hsiao, H. C. Lin, F. H. Ko, Y. S. Yang, *Biosens. Bioelectron.* **2009**, *24*, 3019.
[12] J. Q. Zhao, S. X. Tang, J. Storhoff, S. Marla, Y. P. Bao, X. Wang, E. Y. Wong, V. Ragupathy, Y. P. Ye, I. K. Hewlett, *BMC Biotechnol.* **2010**, *10*, 74.
[13] W. A. Lai, C. H. Lin, Y. S. Yang, M. S. C. Lu, *Biosens. Bioelectron.* **2012**, *35*, 456.
[14] L. Krejcova, D. Hynek, P. Kopel, M. A. M. Rodrigo, V. Adam, J. Hubalek, P. Babula, L. Trnkova, R. Kizek, *Viruses* **2013**, *5*, 1719.
[15] D. Klostermeier, P. Sears, C. Wong, D. P. Millar, J. R. Williamson, *Nucleic. Acids. Res.* **2004**, *32*, 2707.
[16] E. A. Jares-Erijman, T. M. Jovin, *Nat. Biotechnol.* **2003**, *21*, 1387.
[17] A. C. Samia, X. Chen, C. Burda, *J. Am. Chem. Soc.* **2003**, *125*, 15736.
[18] K. Kurokawa, A. Takaya, K. Terai, A. Fujioka, M. Matsuda, *Acta. Histochem. Cytoc.* **2004**, *37*, 347.
[19] K. Aoki, N. Komatsu, E. Hirata, Y. Kamioka, M. Matsuda, *Cancer. Sci.* **2012**, *103*, 614.
[20] L. M. Yao, J. Zhou, J. L. Liu, W. Feng, F. Y. Li, *Adv. Funct. Mater.* **2012**, *22*, 2667.
[21] M. Haase, H. Schäfer, *Angew. Chem. Int. Ed.* **2011**, *50*, 5808.
[22] S. L. Dai, C. X. Li, P. P. Yang, J. Lin, *Chem. Rev.* DOI: 10.1021/cr4001594.
[23] P. A. Ma, H. H. Xiao, X. X. Li, C. X. Li, Y. L. Dai, Z. Y. Cheng, X. B. Jing, J. Lin, *Adv. Mater.* **2013**, *25*, 4898.
[24] Y. Dai, H. Xiao, J. Liu, Q. Yuan, P. Ma, D. Yang, C. Li, Z. Cheng, Z. Hou, P. Yang, J. Lin, **2013**, *135*, 18920.
[25] Z. Li, Y. Zhang, *Angew. Chem.* **2006**, *118*, 7896.
[26] K. W. Krämer, D. Biner, G. Frei, H. U. Güdel, M. P. Hehlen, S. R. Lüthi, *Chem. Mater.* **2004**, *16*, 1244.
[27] C. Zhang, P. Ma, C. Li, G. Li, S. Huang, D. Yang, M. Shang, X. Kang, J. Lin, *J. Mater. Chem.* **2011**, *21*, 717.
[28] S. Zeng, M. Tsang, C. Chan, K. Wong, B. Fei, J. Hao, *Nanoscale* **2012**, *4*, 5118.
[29] R. Deng, X. Xie, M. Vendrell, Y. Chang, X. Liu, *J. Am. Chem. Soc.* **2011**, *133*, 20168.
[30] Z. Chen, H. Chen, H. Hu, M. Yu, F. Li, Q. Zhang, Z. Zhou, T. Yi, C. Huang, *J. Am. Chem. Soc.* **2008**, *130*, 3023.
[31] Q. Ju, Y. Liu, D. Tu, H. Zhu, R. Li, X. Chen, *Chem. Eur. J.* **2011**, *17*, 8549.
[32] D. Tu, L. Liu, Q. Ju, Y. Liu, H. Zhu, R. Li, X. Chen, *Angew. Chem. Int. Ed.* **2011**, *50*, 6306.
[33] S. Zeng, M. Tsang, C. Chan, K. Wong, J. Hao, *Biomaterials* **2012**, *33*, 9232.
[34] P. K. Jain, K. S. Lee, I. H. El-Sayed, M. A. El-Sayed, *J. Phys. Chem. B.* **2006**, *110*, 7238.
[35] G. P. Acuna, M. Bucher, I. H. Stein, C. Steinhauer, A. Kuzyk, P. Holzmeister, R. Schreiber, A. Moroz, F. D. Stefani, T. Liedl, F. C. Simmel, P. Tinnefeld, *ACS Nano* **2012**, *6*, 3189.
[36] Y. Chen, X. Gu, C. Nie, Z. Jiang, Z. Xie, C. Lin, *Chem. Commun.* **2005**, *33*, 4181.
[37] L. Xiong, T. Yang, Y. Yang, C. Xu, F. Li, *Biomaterials* **2010**, *31*, 7078.
[38] J. Zhou, M. Yu, Y. Sun, X. Zhang, X. Zhu, Z. Wu, D. Wu, F. Li, *Biomaterials* **2011**, *32*, 1148.

[39] S. Liu, G. Chen, T. Y. Ohulchanskyy, M. T. Swihart, P. N. Prasad, *Theranostics* **2013**, *3*, 275.
[40] S. Alex, P. Dupuis, *Inorg. Chim. Acta.* **1989**, *157*, 271.
[41] J. L. Liu, Y. Liu, Q. Liu, C. Y. Li, L. N. Sun, F. Y. Li, *J. Am. Chem. Soc.* **2011**, *133*, 15276.
[42] L. M. Yao, J. Zhou, J. L. Liu, W. Feng, F. Y. Li, *Adv. Funct. Mater.* **2012**, *22*, 2667.
[43] R. M. Clegg, Förster resonance energy transfer- FRET what it is, why do it, and how it's done. Lab. Tech. Biochem. Mol. Biol, Vol. *33* (Eds: T. W. J. Gadella), Amsterdam, Elsevier. **2009**, pp. 1–57.
[44] K. C. Grabar, R. G. Freeman, M. B. Hommer, M. J. Natan, *Anal. Chem.* **1995**, *67*, 735.

Received: December 7, 2013
Revised: January 9, 2014
Published online:

DOI: 10.1002/smll.201303766